Journal of Molecular Catalysis A: Chemical 356 (2012) 165–170

Contents lists available at SciVerse ScienceDirect

Journal of Molecular Catalysis A: Chemical

journal homepage: www.elsevier.com/locate/molcata

First-principles study of the methyl formate pathway of methanol steam reforming on PdZn(1 1 1) with comparison to Cu(1 1 1)

Sen Lin[a,*], Daiqian Xie[b], Hua Guo[c]

[a] Research Institute of Photocatalysis, Fujian Provincial Key Laboratory of Photocatalysis-State Key Laboratory Breeding Base, Fuzhou University, Fuzhou 350002, China
[b] Institute of Theoretical and Computational Chemistry, Key Laboratory of Mesoscopic Chemistry, School of Chemistry and Chemical Engineering, Nanjing University, Nanjing 210093, China
[c] Department of Chemistry and Chemical Biology, University of New Mexico, Albuquerque, NM 87131, USA

ARTICLE INFO

Article history:
Received 11 November 2011
Received in revised form 14 January 2012
Accepted 14 January 2012
Available online 24 January 2012

Key words:
Methanol steam reforming
Methyl formate
DFT
PdZn(1 1 1)

ABSTRACT

Methanol steam reforming (MSR), catalyzed by the PdZn alloy, produces hydrogen gas and carbon dioxide with high selectivity. However, the mechanism for MSR has not been completely elucidated. It has been proposed that formate and methyl formate are possible intermediates in MSR. In this study, plane-wave density functional theory was used to investigate the role of methyl formate in MSR on PdZn. It is shown that methyl formate can indeed be formed by a reaction between formaldehyde and methoxyl. In the presence of surface OH species, methyl formate can further react to form formic acid, which can finally dehydrogenate to produce CO_2. However, our calculations show that this hydrolysis process might have difficulties competing with desorption of methyl formate, which is weakly adsorbed on the PdZn surface. Our calculated results thus suggest a minor role for the methyl formate pathway in MSR. Interestingly, the methyl formate reaction pathway shares many similarities with the same process on copper, which is the traditional catalyst for MSR. The insights gained by studying the reaction mechanism on these two surfaces shed valuable light on designing future catalysts for the MSR process.

1. Introduction

Hydrogen based proton exchange membrane (PEM) fuel cells provide a highly efficient and environmentally friendly solution to future transportation and mobile power needs of the post-model society, but their popularization has been fraught with difficulties, partly because of the unsolved problem of hydrogen storage and transportation. A possible solution is to generate hydrogen on board and on demand, using, for example, methanol steam reforming (MSR) [1–3]:

$$CH_3OH + H_2O \rightarrow 3H_2 + CO_2 \quad \Delta H^\circ = 49.6\,kJ/mol.$$

The use of methanol as a hydrogen carrier has a number of advantages [4]. First, it is a liquid fuel which can be readily stored and transported using the infrastructure for the existing transportation fuels with minor modifications. Second, the technology for large scale production of methanol from other feedstocks, including CO_2, is well established and industrial capacity exists. Finally, it is a relatively clean fuel, with a high H/C ratio and no sulfur or nitrogen; and it is miscible with water and biodegradable.

MSR can be realized with a number of catalysts [1,2]. The traditional catalyst is copper dispersed on oxide support. This catalyst has high selectivity toward CO_2, producing only a very small amount of CO. This is important because anodes of PEM fuel cells do not tolerate CO very well. However, the copper catalyst has a few undesirable features, including low thermal stability due to metal sintering and pyrophoricity. For these reasons, there is a strong desire for more stable and equally active and selective MSR catalysts. A recently discovered alternative catalyst of MSR, PdZn, has been shown to have much better thermal stability while maintains the high efficiency and selectivity [5–10]. This discovery has stimulated many recent research activities on the new catalyst [11–17]. There have been some suggestions that the two catalysts have similar electronic properties and might share the same catalytic mechanism [18–20]. However, detailed evidence is still sketchy.

A better understanding of the catalytic mechanism of MSR is important for the design of new and more efficient catalysts. To this end, several reaction pathways have been proposed [7,21]. All these proposed mechanisms assume that MSR is initiated by O—H bond cleavage in both methanol and water, producing adsorbed methoxyl (CH_3O^*) and hydroxyl (OH^*) species, respectively. The catalysis is limited by the dehydrogenation of chemisorbed methoxyl to formaldehyde (CH_2O^*), an assumption supported by both experimental [22–25] and theoretical evidence [26–33]. The surface formaldehyde is known to be a key intermediate in MSR

* Corresponding author.
E-mail address: slin@fzu.edu.cn (S. Lin).

1381-1169/$ – see front matter © 2012 Elsevier B.V. All rights reserved.
doi:10.1016/j.molcata.2012.01.011

[7,9,34], and its further transformations branch out to various other intermediates and products. Several recent theoretical studies have revealed that the reaction of formaldehyde with hydroxyl species on both Cu and PdZn surfaces dominates over the desorption and other reaction channels [33,35,36], including the one that leads to the CO production via the dehydrogenation of formaldehyde [26,27]. The subsequent steps result in various intermediates, such as formate (CHOO*), formic acid (CHOOH*) and dioxomethylene (CH_2OO^{**}), and eventually the production of CO_2 and H_2. Based on these theoretical results, it is now recognized that the reaction between formaldehyde and hydroxyl, while not rate limiting, is the key for the observed selectivity with both Cu and PdZn [33,35]. In addition, our recent DFT studies have demonstrated that the subsequent steps initiated by this reaction are indeed quite similar on the Cu and PdZn surfaces [36].

An alternative MSR pathway involving methyl formate ($CHOOCH_3$) has been proposed by several authors [21,23,34,22], based on the observation that this molecule has been found to desorb from Cu and PdZn surfaces if insufficient steam is provided [7,37,38]. It was also reported that the steam reforming of methyl formate also produces the same CO_2 product as in MSR, even with higher rate [37]. However, the intermediacy of methyl formate in MSR is not supported by diffuse reflectance infrared Fourier transform spectroscopy (DRIFT) experiments by Peppley et al. [23] and more recently by Frank et al. [21], who found no methyl formate on the surface of copper catalysts under normal MSR conditions. Interestingly, the latter did detect signatures of methoxyl, hydroxyl, and formate, which support the formate mechanism discussed above. To resolve this controversy, we have recently shown using plane-wave density functional theory (DFT) that the methyl formate pathway is of minor importance in MSR on Cu, because the reaction of methyl formate with hydroxide cannot compete with that between formaldehyde and hydroxyl [39]. In the current work, we explore this pathway on a PdZn surface using the same plane-wave DFT method [40]. As our results suggest, the reaction steps on PdZn(1 1 1) are similar to those on Cu(1 1 1) and we thus conclude that the methyl formate species are not extensively involved in MSR on PdZn catalyst either.

2. Theory

The PdZn catalyst is modeled in this work by a slab of 1:1 PdZn alloy. This is a reasonable approximation as the PdZn alloy has been identified as the active phase of the catalysis. We will focus here on the (1 1 1) face of the crystal, which is known to be the most stable among various crystal faces of PdZn [18]. Like in our previous work [32,35], all calculations were carried out based on the periodic DFT calculations by using the Vienna ab initio simulation package (VASP) [41–43] with the gradient-corrected PW91 exchange-correction functional [44]. For valence electrons a plane-wave basis set was employed with a cut-off of 400 eV and the ionic cores were described with the projector augmented-wave (PAW) method [45,46]. A $3 \times 3 \times 1$ Monkhorst–Pack k-point grid was adopted to sample the Brillouin zone [47], which was tested to be sufficiently accurate for all the calculations. The Fermi level was smeared using the Methfessel–Paxton method with a width of 0.1 eV [48].

Bulk crystal optimization yielded lattice parameter of $a = b = 4.139$ Å, $c = 3.378$ Å for PdZn, in good agreement with the previously reported results [18]. Slab model for the PdZn(1 1 1) surface consisted of four layers of a 4×4 unit cell with the top layer relaxed in all calculations. A vacuum spacing of 14 Å was used and all adsorbates were placed on one side of the slab.

The adsorption energy was calculated as follows: $E_{ads} = E(\text{adsorbate + surface}) - E(\text{free molecule}) - E(\text{free surface})$. The climbing image nudged elastic band (CI-NEB) method [49,50] was used to determine the transition states with the conventional energy (10^{-4} eV) and force (0.05 eV/Å) convergence criteria. Stationary points were confirmed by normal mode analysis using a displacement of 0.02 Å and an energy convergence criterion of 10^{-6} eV; and the vibrational frequencies were used to compute zero-point energy (ZPE) corrections.

3. Results

3.1. Adsorption

Since many surface species involved in the initial steps of MSR have already been investigated on PdZn(1 1 1) using the plane-wave DFT method [27,28,32,36], we here only focus on the pertinent species in latter steps. The adsorption energies and geometries of the preferred adsorption configurations for several key species are listed in Table 1.

Our calculations indicate that methyl formate adsorbs above the Pd_2Zn_2 parallelogram with its carbonyl oxygen on the top of Zn atom. In addition, two of the hydrogens in the methyl group are pointing to two Pd atoms. This adsorption pattern is consistent with previous theoretical findings that the electronegative oxygen species prefers the zinc site. This closed-shell species has a small adsorption energy of −0.13 eV on PdZn(1 1 1), similar to that found on Cu(1 1 1) [39,51]. Note that DFT is not known to give accurate description of dispersion forces, so the calculated adsorption energy should not be considered to be quantitatively accurate.

The unsaturated species in Table 1 all bind to the PdZn surface with much larger adsorption energies. Unlike the homogenous Cu surface, the heterogeneous PdZn surface offers two distinct active sites. Generally, the electron rich oxygen moiety has a preference on the zinc site while the electron poor carbon and hydrogen moieties prefer to stick to Pd sites. For example, CH_3* preferentially adsorbs on the top of Pd through its carbon atom. The distance between the C atom and surface Pd atom is 2.14 Å. The binding energy was found to be −1.40 eV, which is very close to that on Cu (−1.42 eV). Similar to Cu(1 1 1), the CH_2OOCH_3* species adsorbs on PdZn(1 1 1) with its carbonyl oxygen at an $PdZn_2$ hollow site with methyl pointing away from the surface as shown in Table 1. Its adsorption energy of −2.07 eV is also close to the value of −2.03 eV on Cu. The distances between the adsorbing O atom and the two surface Zn atoms are 2.07 Å, while the length of Pd—O is about 2.39 Å. The C—O—C and O—C—O angles were found to be 114.65° and 112.42°, respectively.

An intermediate species from the dehydrogenation of $CHOOCH_3$*, namely, $CHOOCH_2$**, adsorbs with its methylene carbon and carbonyl oxygen on the top of Pd and Zn atoms, respectively. The adsorption energy of this species is −1.31 eV, which is somewhat larger than that on Cu (−0.84 eV). Finally, the reaction of OH* and $CHOOCH_3$* leads to the generation of the $CHOOHOCH_3$** species. Similar to Cu(1 1 1), $CHOOHOCH_3$** also has two possible adsorption configurations on PdZn(1 1 1), namely, $CHOOHOCH_3$(I)** and $CHOOHOCH_3$(II)**. The former species adsorbs through the hydroxyl oxygen on the top of a Pd atom and another carboxylate oxygen atom at the Zn–Zn short bridge site, as shown in Table 1. The distance between hydroxyl oxygen and Pd atom is found to be 2.50 Å and the lengths of Zn—O (bridge site) are 2.08 and 2.10 Å, respectively. The three O—C—O angles are calculated to be 110.75°, 104.75° and 112.79°, respectively, which is almost equal to those on Cu (110.61°, 104.16° and 113.46°) and the C—O—C angle turns to be 114.33°, slightly larger than the value of 113.42° on Cu. Different from $CHOOHOCH_3$(I)**, $CHOOHOCH_3$(II)** interacts with PdZn(1 1 1) surface through methoxyl O on the top of Pd atom and a carboxylate oxygen at the short Zn–Zn bridge site. Furthermore, the three O—C—O angles become to be 113.51°,

Table 1
Preferred adsorption site and adsorption energy for various pertinent species on PdZn(1 1 1) with comparison to Cu(1 1 1) [39]. Entries in the parentheses are the ZPE-corrected values. Atoms are color labeled: Pd (dark blue), Zn (light blue), O (red), C (black), and H (white).

Species	Adsorption configuration	Adsorption energy (eV)	Adsorption energy on Cu (eV)	Geometry
CH_3	Pd top through C	−1.51 (−1.40)	−1.50 (−1.42)	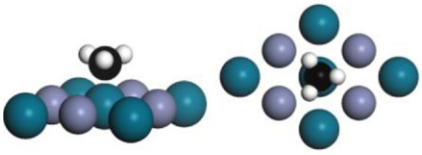
CH_2OOCH_3	$PdZn_2$ hollow through O	−2.22 (−2.07)	−2.18 (−2.03)	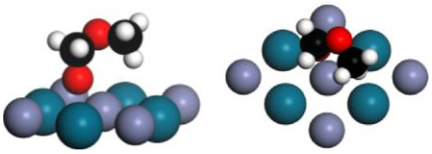
$CHOOCH_3$	Pd_2Zn_2 parallelogram with O on Zn top	−0.14 (−0.13)	−0.07 (−0.06)	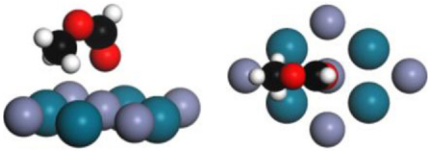
$CHOOCH_2$	Pd–Zn bridge through C and O	−1.41 (−1.31)	−0.93 (−0.84)	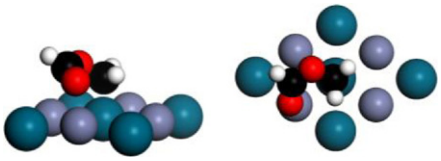
$CHOOHOCH_3$(I)	$PdZn_2$ hollow with one O on Zn–Zn short bridge and the hydroxyl O on Pd top	−2.45 (−2.33)	−2.51 (−2.39)	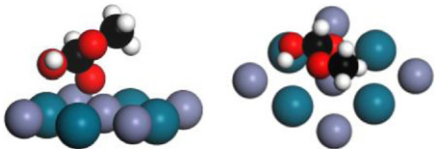
$CHOOHOCH_3$(II)	$PdZn_2$ hollow with one O on Zn–Zn short bridge and the methoxyl O on Pd top	−2.49 (−2.37)	−2.58 (−2.45)	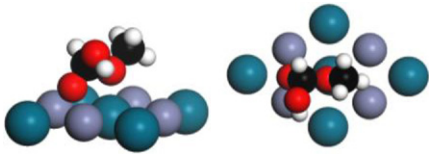

110.80° and 106.02°, respectively and the C—O—C angle extends to 115.37°. In addition, this species has the H of the hydroxyl group points to the surface, as shown in Table 1. The adsorption energies for the last two species (−2.33 and −2.37 eV) are also close to those on Cu(1 1 1), namely, −2.39 and −2.45 eV. As shown in Table 1 our theoretical results indicate that the adsorption of various species on PdZn(1 1 1) and Cu(1 1 1) shares many similarities.

3.2. Reactions

To be complete, we have chosen to reinvestigate the decomposition pathway of adsorbed methanol on PdZn(1 1 1). The barriers and exothermicities for the following four dehydrogenation reactions:

$$CH_3OH^* + * \rightarrow CH_3O^* + H^* \quad (R1)$$

$$CH_3O^* + * \rightarrow CH_2O^* + H^* \quad (R2)$$

$$CH_2O^* + * \rightarrow CHO^{**} + H^* \quad (R3)$$

$$CHO^* + * \rightarrow CO^* + H^* \quad (R4)$$

are listed in Table 2 with ZPE-corrected values in parentheses. Our results are in generally good agreement with previous DFT studies [27,32,52]. In particular, we note that the dehydrogenation of methoxyl has a large (1.24 eV) barrier, which is close to the literature value of 1.17 eV [27]. The high barrier is also consistent with experimental observations that the methoxyl dehydrogenation is the rate-limiting step in MSR.

We are primarily interested in the elementary steps initiated by the reaction between the surface formaldehyde and methoxyl. In particular, the following reactions have been examined:

$$CH_2O^* + CH_3O^* \rightarrow CH_2OOCH_3{}^* + * \quad (R5)$$

$$CH_2OOCH_3{}^* + * \rightarrow CHOOCH_3{}^* + H^* \quad (R6)$$

$$CHOOCH_3{}^* + OH^* \rightarrow CHOOH^* + CH_3O^* \quad (R7)$$

$$CHOOCH_3{}^* + * \rightarrow CHOOCH_2{}^* + H^* \quad (R8)$$

$$CHOOCH_3{}^* + * \rightarrow CHOO^{**} + CH_3{}^* \quad (R9)$$

Table 2
Calculated activation energies and exothermicities (in eV) for reaction steps in methanol decomposition on PdZn(1 1 1).

No.	Elementary reaction	$E^{\neq}$	ΔE
R1	$CH_3OH^* + * \rightarrow CH_3O^* + H^*$	0.94(0.74)	0.09(−0.05)
R2	$CH_3O^* + * \rightarrow CH_2O^* + H^*$	1.24(1.05)	0.93(0.78)
R3	$CH_2O^* + * \rightarrow CHO^* + H^*$	0.89(0.71)	0.19(0.04)
R4	$CHO^* + * \rightarrow CO^* + H^*$	0.44(0.28)	−0.45(−0.60)

Table 3
Calculated activation and reaction energies (eV) for several elementary reactions on PdZn(1 1 1) studied in this work. Entries in the parentheses are the ZPE-corrected values.

No.	Elementary reaction	$E^{\neq}$	ΔE
R5	$CH_2O^* + CH_3O^* \rightarrow CH_2OOCH_3^*$	0.34(0.33)	−0.70(−0.56)
R6	$CH_2OOCH_3^* \rightarrow CHOOCH_3^* + H^*$	1.09(0.90)	−0.05(−0.21)
R7-a	$CHOOCH_3^* + OH^* \rightarrow CHOOHOCH_3(I)^{**}$	0.47(0.52)	0.34(0.40)
R7-b	$CHOOHOCH_3(I)^{**} \rightarrow CHOOHOCH_3(II)^{**}$	0.08(0.08)	−0.08(−0.07)
R7-c	$CHOOHOCH_3(II)^{**} \rightarrow CHOOH^* + CH_3O^*$	0.59(0.49)	−0.34(−0.42)
R8	$CHOOCH_3^* \rightarrow CHOOCH_2^* + H^*$	1.11(0.96)	0.70(0.56)
R9	$CH_2OOCH_3^* \rightarrow CH_2OO^{**} + CH_3^*$	2.13(1.94)	−0.29(−0.39)

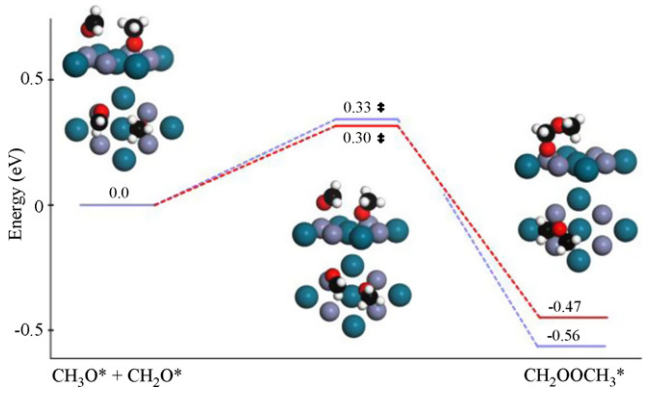

Fig. 1. Energetics (blue) and geometries of IS, TS and FS involved in (R5) on PdZn(1 1 1). The results on Cu(1 1 1) are given in red for comparison. (For interpretation of the references to color in this figure legend, the reader is referred to the web version of the article.)

We did not include two other reactions studied in our previous work on copper [39]. One is the reaction between methyl formate and adsorbed surface oxygen, and the other is the hydrogen abstraction reaction of $CH_2OOCH_3^*$ by OH*. The former is expected to be of minor importance because of the low population of the O* species under MSR conditions. The latter was deemed unimportant in our earlier work because of its high barrier. In addition, the final dehydrogenation reaction for formate:

$$CHOO^{**} \rightarrow CO_2^* + H^* \quad (R10)$$

has been investigated in another publication of ours [36], and thus not repeated here.

The barriers and exothermicities for these elementary reactions on PdZn(1 1 1) are listed in Table 3, with the ZPE-corrected values in parentheses. The geometries of the initial state (IS), transition states (TSs), and the final state (FSs) are depicted in Figs. 1–5. For comparison, the barriers and exothermicities of the corresponding

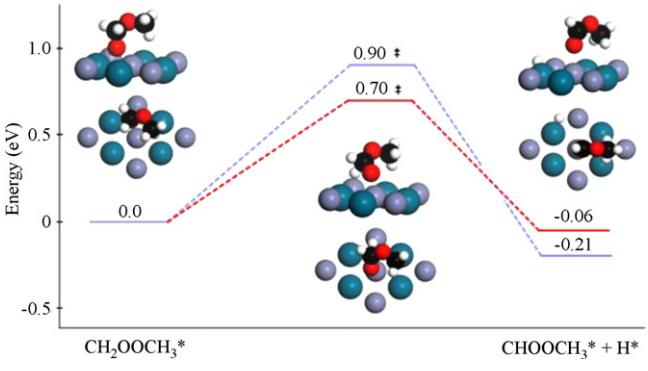

Fig. 2. Same as Fig. 1 for (R6).

reactions on Cu(1 1 1) are also included. A more detailed discussion of all the reaction steps is given below

$$CH_2O^* + CH_3O^* \rightarrow CH_2OOCH_3^* + *$$

This reaction is the initial step in the formation of methyl formate. As discussed below, it only becomes viable in the absence of OH*. At the initial state, the CH_3O^* species binds at a $PdZn_2$ hollow site with its oxygen while the formaldehyde is loosely bound above the PdZn(1 1 1) surface, as shown in Fig. 1. After reaction, $CH_2OOCH_3^*$ also adsorbs at the $PdZn_2$ hollow site with its oxygen. The relatively low barrier of 0.33 eV is very close to 0.30 eV on Cu(1 1 1) and the exothermicity of −0.56 eV is also similar to that on Cu (−0.47 eV) [36].

$$CH_2OOCH_3^* + * \rightarrow CHOOCH_3^* + H^*$$

As shown in Fig. 2, this reaction has a substantial barrier of 0.90 eV, which is 0.20 eV higher than the corresponding barrier on Cu(1 1 1) [36]. In addition, it is found to be −0.15 eV more exothermic on PdZn [36]. At the transition state, the distance of the breaking C—H bond is calculated to be 1.70 Å. After dehydrogenation, the closed-shell product $CHOOCH_3^*$ interacts weakly with the PdZn surface through its carbonyl O atom and the H atom moves to its preferred Pd_2Zn hollow site.

$$CHOOCH_3^* + OH^* \rightarrow CHOOH^* + CH_3O^*$$

Similar to the corresponding reaction on Cu(1 1 1) [39,51], this reaction has multiple steps on PdZn(1 1 1), involving the $CHOOHOCH_3$ intermediate. In the first step (R7-a), the OH* attacks at the carbonyl carbon of methyl formate and the $CHOOHOCH_3(I)^*$ forms along the Zn row through one of its oxygen at the short Zn–Zn bridge site. The barrier and exothermicity are calculated to be 0.52 eV and 0.40 eV, respectively. In the second step, namely R7-b, a change of the adsorption pattern takes place from $CHOOHOCH_3(I)^*$ to $CHOOHOCH_3(II)^{**}$, which has a low barrier of 0.08 eV and is nearly thermoneutral. This step is necessary to adjust the adsorbate for its subsequent dissociation. In the final step, denoted as R7-c, $CHOOHOCH_3(II)^{**}$ decomposes into CH_3O^* and CHOOH* with a barrier of 0.49 eV and the exothermicity is −0.42 eV. After dissociation, the methoxyl located at the preferred $PdZn_2$ hollow site and CHOOH* weakly interacts with a surface Zn atom through its carbonyl O atom. As shown in Fig. 3, the energetics for the reactions are very close to those on Cu(1 1 1) [36,51]. The overall barrier for this step is 0.82 eV.

$$CHOOCH_3^* + * \rightarrow CHOOCH_2^* + H^*$$

As shown in Fig. 4, the dehydrogenation of $CHOOCH_3^*$ to $CHOOCH_2^*$ has a barrier of 0.96 eV, which is 0.47 eV lower than that on Cu(1 1 1) [36]. For the endothermicity, it is 0.30 eV smaller on PdZn than on Cu. After the C—H bond cleavage, the H* species moves to a Pd_2Zn hollow site and $CHOOCH_2^{**}$ adsorbs in a bidentate fashion with C on the top of Pd atom and O on the top of Zn, respectively.

$$CHOOCH_3^* + * \rightarrow CHOO^{**} + CH_3^*$$

The decomposition of $CHOOCH_3^*$ into $CHOO^{**}$ and CH_3^* has a very unfavorable barrier of 1.94 eV, as shown in Fig. 5, similar to that on Cu [36]. Interestingly, at the transition state, the distance between C of CH_3 moiety and oxygen is found to be 2.32 Å, which is very close to that on Cu (2.29 Å). After reaction, CH_3^* locates at the top of Pd, and $CHOO^{**}$ adsorbs with each oxygen atom on the top of Zn.

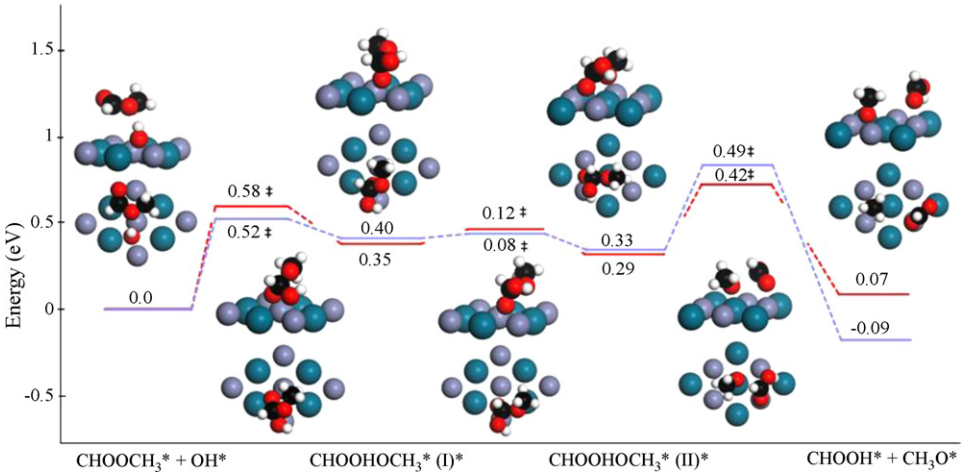

Fig. 3. Same as Fig. 1 for (R7).

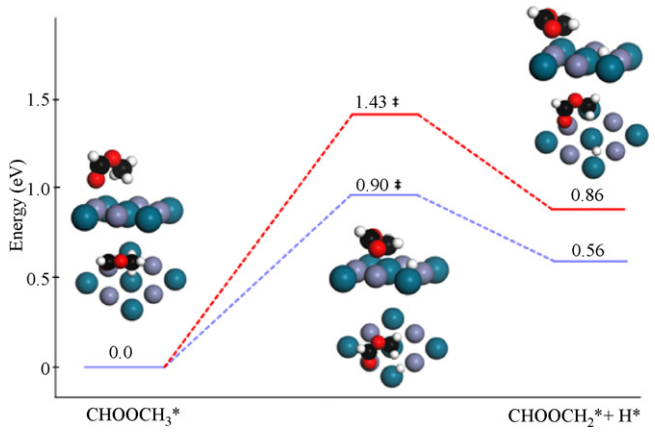

Fig. 4. Same as Fig. 1 for (R8).

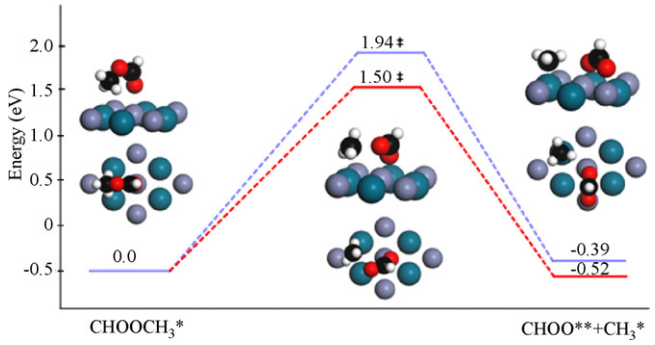

Fig. 5. Same as Fig. 1 for (R9).

4. Discussion

As reported before [36], the reaction between formaldehyde and hydroxyl on PdZn has a very low barrier (0.16 eV) and large exothermicity (−0.34 eV), and this reaction pathway eventually leads to the CO_2 product. The barrier for this reaction is much lower than that of R3 ($E^{\neq}$ = 0.71 eV), which leads eventually to CO. This difference in the reaction barriers, which has also been found on Cu(1 1 1) [33,35], explains the selectivity of both catalysts toward the CO_2 product. It has also been argued that the low barrier allows the reaction to compete effectively with the desorption of formaldehyde [35,36], which is estimated to be 0.61 eV on Cu based on TPD data [53].

The activation barrier for the reaction between formaldehyde and methoxyl (R5) is 0.33 eV, significantly higher than that for the reaction between formaldehyde and hydroxyl. As a result, this channel only becomes important if water (and thus OH*) is absent or at low concentrations. Under such circumstances, it is indeed a facile reaction, because it has a much lower barrier than the dehydrogenation of formaldehyde (R3), while still competitive with its desorption. The situation here is qualitatively the same as on Cu(1 1 1) [39] and is consistent with the experimental observation that methyl formate is formed only when steam is absent [7,8,54]. Once the adduct CH_2OOCH_3 is formed, it proceeds to methyl formate, which can desorb and further react via several possible channels, namely (R7)–(R9), which have respectively barriers of 0.82, 0.96, and 1.94 eV. The barrier for its hydrogenation to CH_2OOCH_3 is also high (1.11 eV). The desorption energy of methyl formate on the PdZn(1 1 1) surface is calculated to be −0.13 eV, but no experimental value is known so far. The theoretical value is almost certainly an underestimation because of the inability of DFT to account for dispersion forces. On Cu, its adsorption energy is estimated to be 0.41 eV from TPD experiments [53], which appears to be a better estimate for the adsorption energy of methyl formate on PdZn. From Table 3, it is clear that all reaction channels have substantial barriers, rendering them unfavorable when comparing with the desorption channel. It is thus likely that methyl formate prefers desorption to further reactions, a conclusion also reached based on theoretical studies on the Cu(1 1 1) surface [39]. However, if methyl formate is fed with steam, it can react to produce $H_2 + CO_2$, along a reaction pathway with no barrier higher than that of the rate-limiting step of MSR.

5. Conclusions

We report in this work a DFT study of the putative methyl formate pathway in MSR on PdZn(1 1 1). Combining with our previous work, we conclude that reactions in the methyl formate pathway on PdZn(1 1 1) surface are quite similar to those on Cu(1 1 1). Both catalytic processes suggested that the methyl formate can indeed be formed via the reaction between formaldehyde and methoxyl in the absence of water (and thus OH*) and react to form the $H_2 + CO_2$ product. However, due to its relatively small adsorption energy relative to all possible reaction barriers, the methyl formate intermediate is likely to desorb rather than react, rendering it of minor importance in MSR.

Acknowledgments

The authors are grateful for the financial support of the New Century Excellent Talents in University of China (NCET-07-0192), National Natural Science Foundation of China (20725312 to DX), a New Direction grant from the Petroleum Research Fund administered by the American Chemical Society (48797-ND6 to HG), and US National Science Foundation (CHE-0910828 to HG). We are grateful to the High Performance Computing Center of Nanjing University for the award of CPU hours to accomplish this work. HG thanks Abhaya Datye for many stimulating discussions.

References

[1] D.L. Trimm, Z.I. Onsan, Catal. Today 43 (2001) 31.
[2] D.R. Palo, R.A. Dagle, J.D. Holladay, Chem. Rev. 107 (2007) 3992.
[3] S. Sa, H. Silva, L. Brandao, J.M. Sousa, A. Mendes, Appl. Catal. B 99 (2010) 43.
[4] G.A. Olah, Catal. Lett. 93 (2004) 1.
[5] N. Iwasa, O. Yamamoto, T. Akazawa, S. Ohyama, N. Takazawa, Chem. Commun. (1991) 1322–1323.
[6] N. Iwasa, S. Masuda, N. Ogawa, N. Takezawa, Appl. Catal. 125 (1995) 145.
[7] N. Takezawa, N. Iwasa, Catal. Today 36 (1997) 45.
[8] N. Iwasa, T. Mayanagi, N. Wataru, T. Takewasa, Appl. Catal. A 248 (2003) 153.
[9] N. Iwasa, N. Takezawa, Top. Catal. 22 (2003) 215.
[10] N. Iwasa, M. Yoshikawa, W. Nomura, M. Arai, Appl. Catal. 292 (2005) 215–222.
[11] Y.-H. Chin, R.A. Dagle, J. Hu, A.C. Dohnalkova, Y. Wang, Catal. Today 77 (2002) 79.
[12] E.S. Ranganathan, S.K. Bej, L.T. Thompson, Appl. Catal. A 289 (2005) 153–162.
[13] E. Jeroro, J.M. Vohs, J. Am. Chem. Soc. 130 (2008) 10199–10207.
[14] C. Rameshan, W. Stadlmayr, C. Weilach, S. Penner, H. Lorenz, M. Havecker, R. Blume, T. Rocha, D. Teschner, A. Knop-Gericke, R. Schlogl, N. Memmel, D. Zembyanov, G. Rupprechter, B. Klotzer, Angew. Chem. Int. Ed. 49 (2010) 3224–3227.
[15] B. Halevi, E.J. Peterson, A. DeLaRiva, E. Jeroro, V.M. Lebarbier, Y. Wang, J.M. Vohs, B. Kiefer, E. Kunkes, M. Havecker, M. Behrens, R. Schlogl, A.K. Datye, J. Phys. Chem. C 114 (2010) 17181–17190.
[16] K. Fottinger, J.A. van Bokhoven, M. Nachtegaal, G. Rupprechter, J. Phys. Chem. Lett. 2 (2011) 428–433.
[17] C. Rameshan, C. Weilach, W. Stadlmayr, S. Penner, H. Lorenz, M. Havecker, R. Blume, T. Rocha, D. Teschner, A. Knop-Gericke, R. Schlogl, D. Zembyanov, N. Memmel, G. Rupprechter, B. Klotzer, J. Catal. 276 (2011) 101–113.
[18] Z.-X. Chen, K.M. Neyman, A.B. Gordienko, N. Rosch, Phys. Rev. B 68 (2003) 1–8.
[19] A.P. Tsai, S. Kameoka, Y. Ishii, J. Phys. Soc. Jpn. 73 (2004) 3270–3273.
[20] A. Bayer, K. Flechtner, R. Denecke, H.-P. Steinruck, K.M. Neyman, N. Rosch, Surf. Sci. 600 (2006) 78.
[21] B. Frank, F.C. Jentoft, H. Soerijanto, J. Krohnert, R. Schlogl, R. Schomacker, J. Catal. 246 (2007) 177.
[22] C.J. Jiang, D.L. Trimm, M.S. Wainwright, N.W. Cant, Appl. Catal. A 93 (1993) 245.
[23] B.A. Peppley, J.C. Amphlett, L.M. Kearns, R.F. Mann, Appl. Catal. A 179 (1999) 31.
[24] J.K. Lee, J.B. Ko, D.H. Kim, Appl. Catal. A 278 (2004) 25.
[25] D.K. Kim, E. Iglesia, J. Phys. Chem. C 112 (2008) 17235.
[26] J. Greeley, M. Mavrikakis, J. Catal. 208 (2002) 291.
[27] Z.-X. Chen, K.M. Neyman, K.H. Lim, N. Rosch, Langmuir 20 (2004) 8068.
[28] Z.-X. Chen, K.H. Lim, K.M. Neyman, N. Rosch, J. Phys. Chem. B 109 (2005) 4568.
[29] S. Sakong, A. Gross, J. Catal. 231 (2005) 420.
[30] S. Sakong, A. Gross, J. Phys. Chem. A 111 (2007) 8814.
[31] D.H. Mei, L.J. Xu, G. Henkelman, J. Phys. Chem. C 113 (2009) 4522.
[32] G.K. Smith, S. Lin, W. Lai, A. Datye, D. Xie, H. Guo, Surf. Sci. 605 (2011) 750.
[33] X.-K. Gu, W.-X. Li, J. Phys. Chem. C 114 (2010) 21539.
[34] K. Takahashi, H. Kobayashi, N. Takezawa, Chem. Lett. (1985) 759.
[35] S. Lin, R.S. Johnson, G.K. Smith, D. Xie, H. Guo, Phys. Chem. Chem. Phys. 13 (2011) 9622.
[36] S. Lin, D. Xie, H. Guo, J. Phys. Chem. C 115 (2011) 20583–20589.
[37] K. Takahashi, N. Takezawa, H. Kobayashi, Appl. Catal. 2 (1982) 363.
[38] I.A. Fisher, A.T. Bell, J. Catal. 184 (1999) 357.
[39] S. Lin, D. Xie, H. Guo, ACS Catal. 1 (2011) 1263–1271.
[40] J. Greeley, J.K. Norskov, M. Mavrikakis, Annu. Rev. Phys. Chem. 53 (2002) 319.
[41] G. Kresse, Hafner, J. Phys. Rev. B 47 (1993) 558.
[42] G. Kresse, Furthmuller, J. Phys. Rev. B 54 (1996) 11169.
[43] G. Kresse, J. Furthmuller, Comput. Mater. Sci. 6 (1996) 15.
[44] J.P. Perdew, J.A. Chevary, S.H. Vosko, K.A. Jackson, M.R. Pederson, D.J. Singh, C. Fiolhais, Phys. Rev. B 46 (1992) 6671.
[45] P. Blochl, Phys. Rev. B 50 (1994) 17953.
[46] G. Kresse, D. Joubert, Phys. Rev. B 59 (1999) 1758.
[47] H.J. Monkhorst, J.D. Pack, Phys. Rev. B13 (1976) 5188.
[48] M. Methfessel, A.T. Paxton, Phys. Rev. B 40 (1989) 3616.
[49] H. Jonsson, G. Mills, K.W. Jacobsen, in: B.J. Berne, G. Ciccotti, D.F. Coker (Eds.), Classical and Quantum Dynamics in Condensed Phase Simulations, World Scientific, Singapore, 1998.
[50] G. Henkelman, H. Jonsson, J. Chem. Phys. 113 (2000) 9978.
[51] L.S. Grabow, M. Mavrikakis, ACS Catal. 1 (2011) 365.
[52] K.H. Lim, Z.-X. Chen, K.M. Neyman, N. Rosch, J. Phys. Chem. B 110 (2006) 14890.
[53] B.A. Sexton, A.E. Hughes, N.R. Avery, Surf. Sci. 155 (1985) 366.
[54] N. Iwasa, T. Akazawa, S. Ohyama, K. Fujikawa, N. Takezawa, React. Kinet. Catal. Lett. 55 (1995) 245–250.